Synthesis and Characterization of $N_3P_3(O_2C_{12}H_8)_2(OC_6H_4Si(CH_3)_3)(OC_6H_4Br)$ and Its Conversion to Nanostructured Si Material

Carlos Díaz · Maria Luisa Valenzuela · Svetlana Ushak

Abstract A new silicated cyclotriphosphazene $N_3P_3(O_2C_{12}H_8)_2(OC_6H_4Si(CH_3)_3)(OC_6H_4Br)$ **1** has been synthesized and characterized. The solid state pyrolysis of **1** in air gives a nanostructured SiP_2O_7 3D network. The morphology of the network strongly depends on the temperature of the pyrolysis. Spinal-like columns and ring-shaped SiP_2O_7 are formed at 800 °C, while, at 600 °C, fused grains of about 300 nm were observed. Based on air TG and DSC thermal studies, we propose the mechanism of formation for the nanostructured network.

Keywords Organometallic derivatives of phosphazenes · Silicon nanostructures · Pyrolysis · Nanomaterials

Introducction

Similarly to polyphosphazenes, cyclophosphazenes have a tremendous variety of applications ranging from lubricants to liquid crystals [1]. However, few derivatives containing silicon substituents have been reported [2–4]. Allcock et al. [2] reported in 1986 the first silicon containing triphosphazenes of the type $N_3P_3Cl_5(R)CH_2Si(CH_3)_3$, R = alkyl. Subsequently, Allcock [3] reported another series of the general formula $N_3P_3(OC_6H_5)_5NH(CH_2)_3Si(CH_3)_2)OSi(CH_3)_3$ and $N_3P_3(OC_6H_5)_5NH(CH_2)_3Si(CH_3)_2Si(OSi(CH_3)_3)_3$. Other silicon derivatives have been also revised by Allcock [4].

C. Díaz (✉) · S. Ushak
Department of Chemistry, Faculty of Science, Universidad de Chile, Casilla 653, Santiago, Chile
e-mail: cdiaz@uchile.cl

M. L. Valenzuela
Departamento de Química Orgánica e Inorgánica. Facultad de Química, Universidad de Oviedo, C/Julián Clavería S/N, Oviedo 33071, Spain

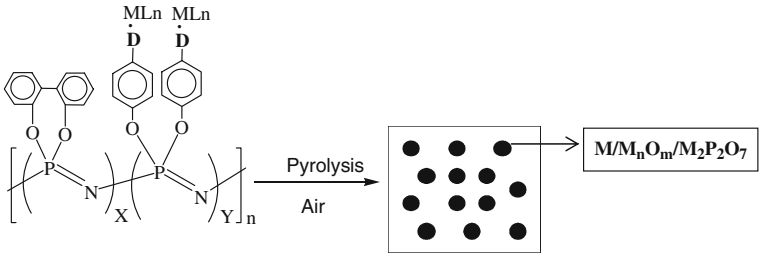

Scheme 1 Schematic representation of the SSPO method

Spirocyclic triphosphazenes are a new class of trimers [5]. Although several cyclic spirophosphazenes of the type $N_3P_3(O_2C_{12}H_8)_{6-2n}R_{2n}$ n = 0, 1 or 2 are known [1], those with the substituent R containing silicon groups are scarce [2–4]. Here we report the synthesis and characterization of $N_3P_3(O_2C_{12}H_8)_2(OC_6H_4Si(CH_3)_3)(OC_6H_4Br)$ **1**.

The development of nanometer sized particles has been intensively pursued due to their technological and fundamental scientific importance [6]. These nanoparticle materials exhibit very interesting electrical, optical, magnetic and chemical properties, which cannot be achieved by their bulk counterparts. Silicon nanostructured materials are of great importance due to their electronic applications [7, 8]. The most widely investigated nanomaterials have been Si and SiO_2, and few other containing silicon nanoparticles have been reported [6].

We have previously reported [9–17] a solid-state pyrolysis of organophosphazene/organometallic (SSPO) method for the production of the metallic nanoparticles and metallic salt nanostructured materials (see scheme 1). This pyrolitic method starts from a polyphosphazene containing an organometallic anchored fragment.

The aim of this work was to investigate if the pyrolysis of an easier to prepare precursor such as a triphosphazene, with respect to the respective polymer, could afford metallic nanostructured materials as showed in scheme 1.

We herein report the production of nanostructured Si containing materials using solid state pyrolysis of the trimer precursor $N_3P_3(O_2C_{12}H_8)_2(OC_6H_4Si(CH_3)_3)(OC_6H_4Br)$, under air atmosphere and at 800 °C.

Experimental

All reactions were carried out under nitrogen using standard Schlenk techniques. Infra-red (IR) spectra were recorded with a FT–IR Perkin–Elmer 2000 spectrophotometer. Solvents were dried and purified using standard procedures. $O_2C_{12}H_{10}$ (biphenol), $ClSi(CH_3)_3$, HOC_6H_4Br, $N_3P_3Cl_6$ and n-BuLi were obtained from Sigma–Aldrich Nuclear magnetic resonance (NMR) spectra were conducted using a Bruker AC-300 instrument with $CDCl_3$ as the solvent unless otherwise stated. ^1H and $^{13}C\{^1H\}$-NMR are given in δ relative to TMS. $^{31}P\{^1H\}$-NMR are given in δ relative to external 85% aqueous H_3PO_4. Coupling constants are in Hz. Thermogravimetric analysis (TGA) and differential scanning calorimetry (DSC) measurements were

performed on a Mettler TA 4000 instrument and Mettler DSC 300 differential scanning calorimeter, respectively. The trimer samples were heated from room temperature to 800 °C with a ramp of 10 °C min^{-1} under a constant nitrogen flow.

Scanning electron microscopy (SEM) and energy dispersive X-ray analysis (EDX) were recorded with a JEOL 5410 SEM with a NORAN Instrument micro-probe transmission microscope. Transmission electron microscopy (TEM) was carried out on a JEOL SX100 TEM. The finely powered samples were dispersed in *n*-hexane and dropped on a conventional carbon-coated copper grid and dried with a lamp.

The pyrolysis experiments were carried out by pouring a weighed portion (0.05–0.15 g) of the organometallic trimer into aluminum oxide crucibles. The samples were placed in a box furnace, previously heated to 300 °C, and annealed for 2 h at 600 °C or 800 °C.

Synthesis of 1

To $N_3P_3(O_2C_{12}H_8)_2(OC_6H_4Br)_2$, 0.835 g (1 mmol), prepared as reported previously[18], in THF 50 mL at—78 °C was added dropwise n-BuLi 6 mL (9.6 mmol) and stirred for 2 h. Then $ClSi(CH_3)_3$ 2.3 mL (18.2 mmol) was added and the solution stirred for 15 h at room temperature. After this water was added and stirrted for 1 h. The excess of water was removed with anhidrous K_2CO_3 and the solvent was evaporated under vacuum and the solid extracted with dichloromethane and filtered thought Celite. Evaporation of the solvent in vacuum gave **1** as a white solid. The solid was recrystallized using a mixture of benzene and acetone. Yield 52 %. Elemental analysis Calc. for $C_{39}H_{33}O_6N_3P_3BrSi \cdot 1/2CH_2Cl_2$ C, 53.7; H, 3.97; N, 4.76. Found C, 53.0; H, 4.24; N, 4.57. MS:m/z = 840.6, M^+, 760.13, M^+ −Br, 766.0, M^+−$Si(CH_3)_3$, 678.51, M^+ −Br, $Si(CH_3)_3$.

IR (KBr pellet) in cm^{-1}, 3067, 2953, 1586, 1482, 1438, 1273 (*v* Si–O), 1231, 1171 (*v* PN), 1093, 971, 949, 985, 838, 786, 755, 610, 522. ^{1}H NMR ($CDCl_3$):*δ* 7.7–7.2 m, arom rings, 0.29 s, CH_3. ^{31}P {^{1}H} NMR($CDCl_3$) 26.38, 26.13, 25.62, 25.37 $P(O_2C_{12}H_8)$; 11.04, 10.87, 10.29, 10.13, 9.51, 9.35 $P(OC_6H_4X)$. J(P–P) 91.18 Hz.

^{13}C NMR {^{1}H} ($CDCl_3$) 150.41, 137,16, 135.02, 132.21,132,10, 131,97, 131.07, 128.63, 128.44, 125.54, 124.26, 124,14, 123.02 ($O_2C_{12}H_8$ and OC_6H_4X); 1.46 (CH_3).

Results and Discussion

Synthesis of the Precursor

The synthesis of precursor $N_3P_3(O_2C_{12}H_8)_2(OC_6H_4Si(CH_3)_3)(OC_6H_4Br)$ **1** was achieved in several steps from the reaction of $N_3P_3Cl_6$ with the biphenol $O_2C_{12}H_{10}$ to give $N_3P_3(O_2C_{12}H_8)_2Cl_2$, which reacts with bromophenol to give $N_3P_3(O_2C_{12}H_8)_2(OC_6H_4Br)_2$ **1a** [18]. This was lithiated with n-BuLi forming a intermediary **1b** and then $ClSi(CH_3)_3$ was added (see scheme 2).

Although in the experimental procedure an excess of n-LiBu was used, the not consumed reactive was deactivated with water. The no obtention of the disilylated product can be due to steric hindrance to enter the second silylated group. The

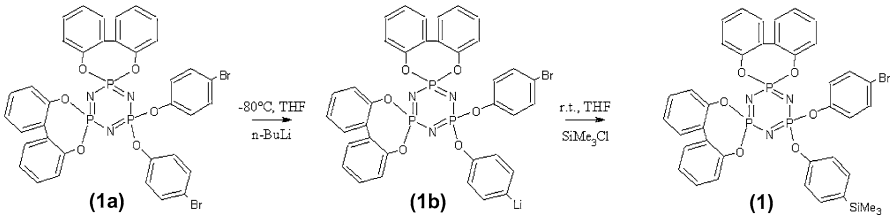

Scheme 2 Synthesis of the trimer $N_3P_3(O_2C_{12}H_8)_2(OC_6H_4Si(CH_3)_3)(OC_6H_4Br)$

product is a white solid which was characterized by elemental analysis, mass spectrometry, ^{1}H, ^{31}P and ^{13}C NMR spectroscopy as well as thermal (TGA and DSC) analyses. The mass spectrum displays the molecular ion at m/e = 841.69 with the expected isotopic distribution corresponding to the presence of Br. Fragmentation of **1**, affords a peak at m/e = 766.006, corresponding to the fragment arising from the loss of the $Si(CH_3)_3$ group from the molecule. On the other hand, the peak observed at m/e = 760.135 can be assigned to the loss of the bromine from the molecule. Thus the mass spectrum of the compound **1** does not exhibit m/e values corresponding to the starting compound neither disilylated product.

The ^{1}H-NMR spectrum exhibits a complex set of signals corresponding to the protons of the bispiro groups at 7.6–7.2 ppm, as well as to the OC_6H_4Br group at 7.07 and 6.96 ppm, with an intensities ratio 3:1, in agreement with the proposed formula. Each of the signals appears doubled, suggesting the presence of all the expected (R,R)-, (S,S)-enantiomeric configurations and the distereotopic meso—forms. In principle, as found in several derivatives of gem-$[N_3P_3(O_2C_{12}H_8)_2(OR)_2]$, the four diasteroisomers could be distinguished by NMR spectroscopy [19–21]. In fact the ^{31}P-NMR signals confirm the presence of all the possible stereoisomers (R,R, S,S S,R, and R,S) that exist in solution. Two sets of resonance peaks were observed, as is shown in Fig. 1, typical of this type of process. Both the position, as well as the splitting expected for a AX_2 spin system, are in agreement with the expected parameters for derivatives of gem-$[N_3P_3(O_2C_{12}H_8)_2(OR)_2]$. Thus the coupling constant of these types of compounds are around 90 Hz [18–21] in agreement with that found for **1**, 91.18 Hz.

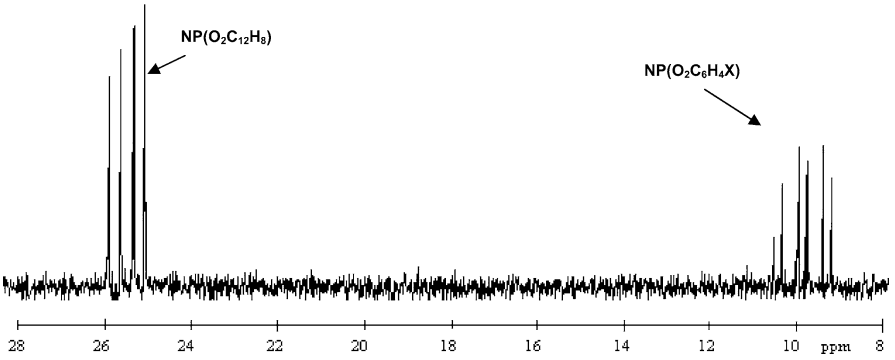

Fig. 1 ^{31}P NMR spectrum of $N_3P_3(O_2C_{12}H_8)_2(OC_6H_4Si(CH_3)_3)(OC_6H_4Br)$

^{13}C-NMR spectra display the expected signals (see experimental part), in particular the signal corresponding to the $Si(CH_3)_3$ group which appears at 1.45 ppm.

The thermogravimetric analysis under N_2 flow shows an initial gradual weight loss of 4.8% between 50 °C and 260 °C, which is due to the loss of volatile species, generated during the condensation reactions.

Above 300 °C the sample exhibits a sharp weight loss of 50.7% in the temperature range of 300–600 °C, which can be explained by the total chemical degradation of the material. The differential scanning calorimetric (DSC) measurement under N_2 exhibits in the temperature range of 0–250 °C an endothermic process, which can be explained by evaporation of the solvent and volatile species discussed in the TG curve. Another endothermic process was observed around 450 °C, which was attributed to the evaporation of volatile species generated during the condensation reactions. Three exothermic effects, between 500 °C and 600 °C, can be assigned to the degradation of the material.

Pyrolysis of the Si Precursor

Pyrolysis of the silane-containing trimeric phosphazene was studied at 600 and 800 °C, in an air atmosphere. The resulting gray pyrolytic residues obtained at 600 and 800 °C were characterized by SEM-EDAX, IR, TEM and XRD. The pyrolytic yields were typically in the range 15–20%; the values are consistent with the residues measured by thermogravimetric analysis up to 800 °C in air, see bellow.

The X-ray powder diffraction pattern of the pyrolytic product from **1** exhibits the presence of SiP_2O_7, in one or several of its known crystalline phases [22]. A typical representative powder diffraction pattern is shown in Fig. 2. In this case two phases are observed: monoclinic and cubic.

Consistently, the IR spectra of the pyrolytic residue from the silicon precursor **1** exhibit absorptions at 1180–1050 cm^{-1} (vs, broad), 800–680 cm^{-1} (w), and 490 cm^{-1} (s, br), in agreement with previous IR and Raman spectra of SiP_2O_7 [23, 24].

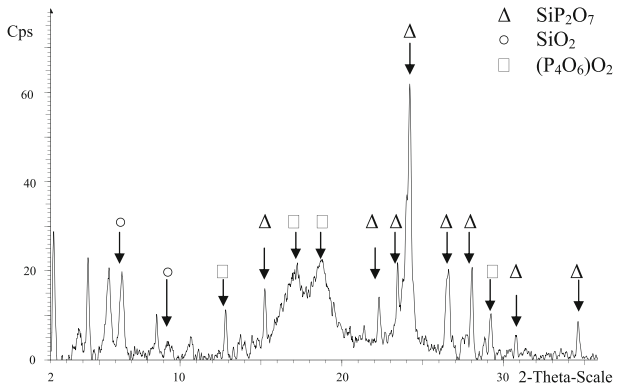

Fig. 2 Diffraction pattern of pyrolytic product at 800 °C

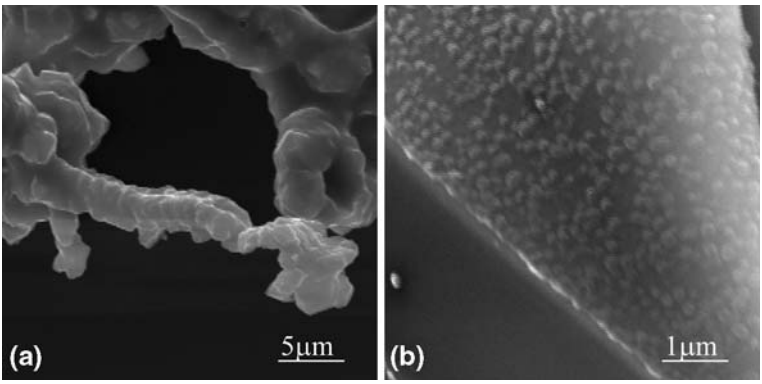

Fig. 3 SEM images for pyrolytic products at (**a**) 800 °C, (**b**) 600 °C

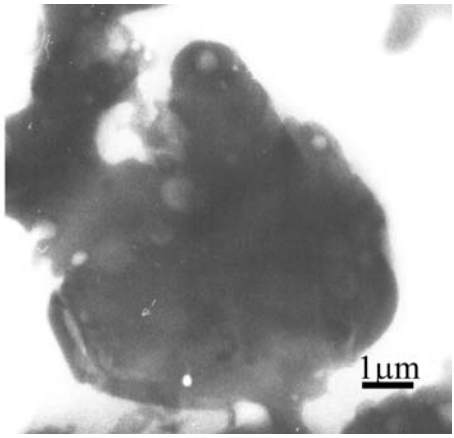

Fig. 4 TEM image of the pyrolysis product obtained from trimer **1** at 800 °C

The SEM images of the residue shown in Fig. 3 exhibit a morphology dependent on the temperature.

At 800 °C an interesting 3D-morphology composed of rings as well as of bars is observed. However, a close inspection of the bars evidences (as the image showed in Fig. 3a) that these are composed of vertebra-like shaped species. Fused granular microstructures of about 500 nm were observed for pyrolytic precursor of **1** obtained at 600 °C. The TEM image in Fig. 4 exhibits somewhat high agglomerates of about 2.5 μm, in agreement with the SEM data discussed above.

Mechanism of Formation of the Nanostructured Silicon Materials

Based on the thermogravimetric data, and previously proposed mechanisms for the formation of metallic nanostructures from pyrolysis of organometallic derivatives of polyphosphazenes [9–17], we propose a formation mechanism of nanostructured SiP_2O_7 from the trimer **1**. The TG curve showed in Fig. 5 exhibits a first small weight loss (4.8%) around 150 °C, associated with a loss of solvent molecules.

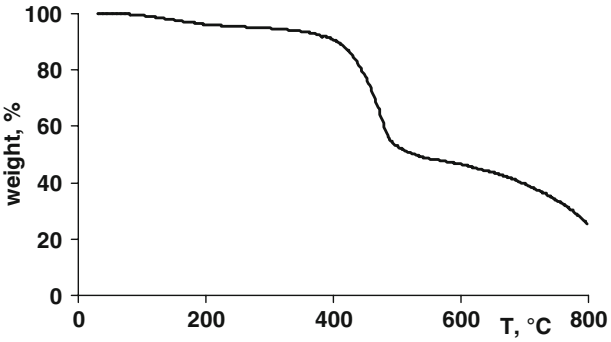

Fig. 5 TG curve of (**1**) under an air atmosphere

Following this, a high weight loss at 450 °C can be assigned to the carbonization of the organic matter (arising from the bispiro as well as the C_6H_4Br groups), with loss of CO_2 (calculated 48.15% versus experimental 48.9%).

Finally a loss of phosphorus and nitrogen oxides as well as CO_2 from the remaining organic matter, affords a residue of 25.08% corresponding to the SiP_2O_7 product (calculated 24.80%). Then, a plausible mechanism for the formation of SiP_2O_7 from pyrolysis of **1** under air could be: the organic moiety, after calcination, produces holes and cross-linking of the cyclophosphazene rings, forming probably cyclomatrix structures. The silicon atoms are released from the trimer rings and probably reduced by the CO, formed by the incomplete combustion of the organic matter. The silicon atoms are re-oxidized in air, forming SiO_2. Simultaneously, phosphorus atoms arising from the inorganic PN backbone of the phosphazene rings are also oxidized forming P_2O_5 and other phosphorus oxides (e.g. P_4O_7). Following this, SiO_2 reacts with P_2O_5 which is known to form SiP_2O_7 at high temperatures [25–31]. As found in previous studies [9–17] the oxide P_4O_7 acts as a stabilizer of the SiP_2O_7 precluding, in some cases, the agglomeration of the particles.

Applications of SiP_2O_7

SiP_2O_7 particles have been used as catalysts in the Fischer–Tropsch refining reactions [32, 33] and as proton conducting materials in fuell cell electrolytes and hydrogen powder cells [34–36]. However, these are non nanostructured SiP_2O_7 materials that have been used in such applications. As in known in the field of the nanocatalysis, nanostructured materials usually gives enhanced catalytic properties [37]. Therefore the above mentioned materials have to be tested as catalysts, in order to verify their catalytic properties.

Conclusions

From readily available starting $N_3P_3(O_2C_{12}H_8)_2(OC_6H_4Br)_2$ precursor, the new cyclic trimer $N_3P_3(O_2C_{12}H_8)_2(OC_6H_4Si(CH_3)_3)(OC_6H_4Br)$ was prepared and

characterized. The structure exhibits all the possible R,R, S,S S,R and RS stereoisomers, due to the twistings the bispiro groups as evidenced by ^{1}H, ^{31}P and ^{13}C NMR spectroscopy.

This type of trimer results to be a useful precursor for the preparation of nanostructured SiP_2O_7, through the pyrolysis at 800 °C under air. The formation mechanism involves the generation of holes, due to the release of CO_2, where the metal centers are formed. Phosphorus oxides act as stabilizers of the solid state nanostructures.

Pyrolysis experiments with other Silicon containing trimer are in course.

Acknowledgement This work was financially suppported by Fondecyt (Project 3060092) and MECESUP Project UCH0116.

References

1. M. Gleria and R. Pager (2004) Applications Aspects of Cyclotriphosphazenes (Nova, 2004)
2. H. R. Allcock, D. J. Brennan, J. M. Graaskamp, and M. Parvez (1986). *Organometallics* **5**, 2435.
3. H. R. Allcock, D. J. Brennan, and D. Beverly (1988). *Macromolecules* **27**, 3226.
4. H. R. Allcock and D. J. Brennan (1988). *J. Organomet. Chem.* **341**, 231.
5. G. A. Carriedo and F. Garcia-Alonso, High molecular weight polyspirophosphazenes. In *Phosphazenes :A World Insight*, eds. R. Jaeger, M. Gleria. Nova Sci. Publ: New York, 2005.
6. C. N. Rao, A. Muller, and A. K. Cheetham, *The Chemistry of Nanomaterials*. Wiley—VCH, 2003.
7. L. Tsybeskov (1998). *MRS. Bull.* **23**, 33 .
8. A. Shah, P. Torres, R. Tscharner, R. Wyrsch, and H. Keppner (1992). *Science* **285**, 692.
9. C. Diaz and M. L. Valenzuela (2005). *J. Chil. Chem. Soc.* **50**, 417.
10. C. Diaz and M. L. Valenzuela (2006). *Macromolecules* **39**, 103.
11. C. Diaz, P. Castillo, and M. L. Valenzuela (2005). *J. Cluster Sci.* **16**, 515.
12. C. Diaz and M. L. Valenzuela (2006). *J. Inorg. Organometallic Polym.* **6**, 123.
13. C. Diaz and M. L. Valenzuela, Coordination of organometallic fragments to polyphosphazene containing side groups with donors atoms. In *Horizons in Polymer Developments*, ed. R. B. Bregg. Nova Science Publishers: NewYork, 2006.
14. C. Diaz, D. Abizanda, J. Jimenez, A. Laguna, and M. L. Valenzuela (2006). *J. Inorg. Organometallic Polym.* **6**, 211.
15. C. Diaz and M. L. Valenzuela (2006). *J. Inorg. Organometallic Polym.* **6**, 419.
16. C. Diaz, M. L. Valenzuela, and N. Yutronic (2007). *J. Inorg. Organomet. Polym.* **17**, 577.
17. C. Diaz, E. Spodine, Y. Moreno, O. Peña, and M. L. Valenzuela (2007). *J. Cluster Science*, **19**, 831.
18. G. A. Carriedo, L. Fernandez-Catuxo, F. J. Garcia-Alonso, P. Gomez-Elipe, and P. A. Gonzalez (1996). *Macromolecules* **29**, 5320.
19. D. Kumar and A. D. Gupta (1995). *Macromolecules* **28**, 6323.
20. I. Dez, J. Levalois-Mitjaville, H. Grutzmacher, V. Gramlich, and R. De Jaeger (1999). *Eur. J. Inorg. Chem.* 1673.
21. A. Vij, J. Geib, R. L. Kirchmeier, and J. M. Shreeve (1996). *Inorg. Chem.* **35**, 2915.
22. D. M. Poojaray, R. B. Borade, F. L. Campbell, and A. Clearfield (1994). *J. Solid State Chem.* **112**, 106.
23. N. Shibata, M. Horigudhi, and T. Edahiro (1981). *J. Non-Crystalline Solids* **45**, 115.
24. J. Wong (1973). *J. Non-Crystalline Solids* **20**, 83.
25. T. V. Kovalchuk, H. Sfihi, A. Korchev, S. Kovalenko, V. N. IÍin, V. G. Zaitzev, and J. Fraissard (2005). *J.Phys. Chem. B* **109**, 13948. doi:10.1021/jp0580625.
26. D. M. Karpinos, E. P. Mikhashchuk, R. A. Amirov, and U. Sh. Shayakhmetov (1982). *Power Meta. Met. Cer.* **21**: 388.
27. S. Suehara, T. Konishi, and S. Inoue (2006). *Phys. Rev.* **B73**, 092203.
28. T. Uma and M. Nogami (2006). *Mater. Chem. Phys.* **98**, 382.
29. J. Roman, S. Padilla, and M. Vallet-Regi (2003). *Chem Mater.* **15**, 798.

30. N. Nishiyama, J. Kaihara, Y. Nishiyama, Y. Egashira, and K. Ueyama (2007). *Langmuir* **23**, 4746.
31. T. Matsui, T. Kukino, R. Kikuchi, and K. Eguchi (2006). *J. Electrochem. Soc.* **157A**, 339.
32. J. H. Coetze, T. N. Mashapa, N. M. Prinsloo, and J. D. Rademan (2006). *Appl. Catal.* **A 308**, 204.
33. T. R. Krawietz, P. Lin, K. E. Lotterhos, P. D. Torres, A. C. Barich, and J. F. Haw (1998). *J. Am. Chem. Soc.* **120**, 8501.
34. T. Matsui, T. Kukino, R. Kikuchi, and K. Eguchi (2006). *Electrochim. Acta* **51**, 3719.
35. Y. Daiko, T. Kasuga, and M. Nogami (2002). *Chem. Mater.* **14**, 4624.
36. M. Nogami, Y. Daiko, T. Akai, and T. Kasuga (2001). *J. Phys. Chem.* **105**, 4653.
37. A. T. Bell (2003). *Science* **299**, 1688.